



# Assessing the Effects of Surface Conditions on Potential Evapotranspiration in a Humid Subtropical Region of China

Hailong Wang<sup>1,2\*</sup> and Jinghua Zheng<sup>1,2</sup>

<sup>1</sup> School of Civil Engineering, Sun Yat-sen University, Guangzhou, China, <sup>2</sup> Southern Marine Science and Engineering Guangdong Laboratory, Zhuhai, China

## OPEN ACCESS

### Edited by:

Xuhui Zhou,  
East China Normal University, China

### Reviewed by:

Fenghui Yuan,  
University of Minnesota Twin Cities,  
United States  
Abu Reza Md. Towfiqul Islam,  
Begum Rokeya University, Bangladesh

### \*Correspondence:

Hailong Wang  
wanghlong3@mail.sysu.edu.cn

### Specialty section:

This article was submitted to  
Climate, Ecology and People,  
a section of the journal  
Frontiers in Climate

Received: 12 November 2021

Accepted: 03 January 2022

Published: 03 February 2022

### Citation:

Wang H and Zheng J (2022)  
Assessing the Effects of Surface  
Conditions on Potential  
Evapotranspiration in a Humid  
Subtropical Region of China.  
Front. Clim. 4:813787.  
doi: 10.3389/fclim.2022.813787

The ability of the atmosphere to remove water from land surface is measured by potential evapotranspiration ( $ET_p$ ), which is often inferred by the reference evapotranspiration ( $ET_o$ ). Therefore,  $ET_p$  is often considered only influenced by the above-ground meteorological conditions. Based on its concept,  $ET_p$  should also link with surface conditions that influence the surface resistance. Such linkages differ in dry and wet regions with different surface covers. Here, we calculated  $ET_o$  and especially analyzed the effects of surface conditions including vegetation cover indicated by NDVI (Normalized Difference Vegetation Index) and root-zone SWC (soil water content) in a humid subtropical province of China. Results show that  $ET_p$ , NDVI, wind speed, temperatures have increased significantly during 1982–2015 and relative humidity (RH) has decreased significantly. Linear trends of these variables varied across seasons, but similarities were found between spring and winter and between summer and autumn. Summer saw the greatest changes in  $ET_p$  per unit of environmental variable change. Solar radiation, RH, and precipitation exerted overall stronger influence on  $ET_p$  ( $R^2 > 0.50$ ) than other factors. NDVI and SWC were found positively and negatively affecting  $ET_p$  at all time scales. Partial correlation analysis showed significant influence of NDVI and SWC at the monthly scale; moreover, SWC influenced  $ET_p$  more significantly in summer than other seasons ( $p < 0.05$ ). Since actual evapotranspiration is often deducted from  $ET_p$  by multiplicative stress functions in many hydrologic models, understanding the relationships between  $ET_p$  and environmental changes can help improve the formulation and estimation of actual evapotranspiration.

**Keywords:** potential evapotranspiration, soil water content, vegetation cover, climate change, time scales

## INTRODUCTION

Potential evapotranspiration ( $ET_p$ ) is defined by many researchers as the water escaping rate from a well-watered vegetated surface (e.g., Xiang et al., 2020). The characteristics of vegetated surface can vary in different definitions, for example, Rosenberg (1974) defined  $ET_p$  as “the evaporation from an extended surface of a short green crop which fully shades the ground, exerts little or negligible resistance to the flow of water, and is always well supplied with water,” in which the vegetation features are implicit; while Allen et al. (1998) defined a reference grass with a fixed height of 0.12 m,

a surface resistance of  $70 \text{ s m}^{-1}$ , and an albedo of 0.23, and hence their ET<sub>p</sub> is also known as the reference evapotranspiration (ET<sub>o</sub>). Therefore, the main difference between ET<sub>p</sub> and ET<sub>o</sub> lies in the parameterization of the surface conditions particularly vegetation type and characteristics. By any definitions, ET<sub>p</sub> measures the ability of the atmosphere to remove water from land surface through evaporation and transpiration (Kirkham, 2014). The two types of evapotranspiration are often considered for practical purposes of water resource management like guiding crop irrigation (Allen et al., 1998; Wen et al., 2016). ET<sub>p</sub> is an indispensable input variable for many land surface models and hydrologic models to compute ET<sub>a</sub> and other water budget components (Chen and Dudhia, 2001; Ala-aho et al., 2017), and plays a significant role in assessing regional dry and wet conditions and variations in meteorological conditions (Vicente-Serrano et al., 2010; Beguería et al., 2014; Yang et al., 2019; Zhang and Wang, 2021; Zhou et al., 2021). Therefore, quantification of ET<sub>p</sub> determines the performance of such models regarding the water flows, mixing and balance to better understand the interactions between climate and hydrology.

So far, various methods for ET<sub>p</sub> quantification have been developed, such as the Thornthwaite model (Thornthwaite, 1948), the Priestley-Taylor equation (Priestley and Taylor, 1972), the Penman-Monteith equation (Monteith, 1965), etc. The current physically based methods can be categorized into four major types, i.e., temperature-based, radiation-based, the combination method, and the mass transfer-based methods (which utilize the fundamentals of Dalton's law and the concept of eddy transfer of water vapor from an evaporating surface to the atmosphere). They have been compared extensively across a wide spectrum of climate and geolocation, and the combination method represented by the Penman-Monteith equation is considered superior to others in general (Lu et al., 2005; Oudin et al., 2005; Fisher et al., 2011; Mallick et al., 2013). Based on these methods a rich pool of ET<sub>p</sub> products have been produced for hydrology and climate research (Rodell et al., 2004; Mu et al., 2007; Miralles et al., 2011; Zhang et al., 2019). It is worth mentioning that more recently, non-physically based soft computing models have also been developed using various machine learning techniques such as these reviewed in Adnan et al. (2021) and Salam and Islam (2020), which have improved both the computing efficiency and simulation accuracy with less demand for input variables.

Composed of evaporation and transpiration, ET<sub>p</sub> is a function of meteorology and the surrounding near-surface environment (Zhan et al., 2019), therefore, ET<sub>p</sub> can vary simultaneously with changes in surface conditions, which has been proved by previous studies. For instance, Yang et al. (2011) claimed that relative humidity was the most influential factor followed by solar radiation and wind speed in the Yellow River Basin, whereas Wang et al. (2014) reported that temperature was the main reason for ET<sub>p</sub> change in a northern China irrigation district, followed by wind speed and relative humidity; Duethmann and Blöschl (2018) found in over 150 Austrian catchments that ET<sub>o</sub> increased with increased net radiation and temperature; Zhang et al. (2020) found temperature and sunshine hours were the two most influential factors in Shandong province, China,

while Jerin et al. (2021) reported the dominant factors for ET<sub>o</sub> were mean temperature, solar duration and relative humidity in Bangladesh. de Oliveira et al. (2021) found solar radiation was the most important factor controlling ET<sub>o</sub> in the southern Amazon basin, same with findings in Valle Júnior et al. (2021). These studies demonstrate that the weight of meteorological variables on ET<sub>p</sub> quantification varies with regions and spatiotemporal scales. Although different in concept between ET<sub>p</sub> and ET<sub>o</sub> (Xiang et al., 2020), the latter is often used as the potential ET in these studies due to its simplicity where vegetation parameters are fixed, and because of this, the impact of vegetation cover is rarely explored and can somewhat be reflected in the near-surface meteorological variables if there is a close interaction between plant and atmosphere. Moreover, ET<sub>p</sub> is considered not limited by water supply by its definition, so the relationship between ET<sub>p</sub> and soil water condition is also not attended to. This assumption leaves meteorology the only factor governing ET<sub>p</sub> changes when using the modified Penman-Monteith equation in the well-known FAO56 paper for the reference grass (Allen et al., 1998; Chu et al., 2017; Li et al., 2018). However, because of the connections in the soil-plant-atmosphere continuum regarding water flow and energy transfer, the divergence in the effects of surface conditions on near-surface meteorology and soil water content (Jiao et al., 2021), and the fact that ET<sub>p</sub> integrates the vegetation impacts through the surface resistance that is influenced by many environmental factors (Zhang et al., 2019; Wang et al., 2020), it is reasonable to hypothesize that ET<sub>p</sub> can be influenced by the changes in vegetation growth and soil water content besides meteorology, which however draws little attention so far and needs further proof and justification.

Moreover, most of the previous studies are focused in the dryland areas where water availability primarily restrains ecosystem development, and atmospheric demand is usually high with high variabilities due to the high seasonal radiation and low vegetation covers (Hua et al., 2020); yet less is known about the variations of ET<sub>p</sub> and its connections with vegetation and soil water content in the humid areas. In a previous study in Guangdong, a humid southern province of China, it was found that ET<sub>p</sub> has decreased by  $\sim 1 \text{ mm yr}^{-1}$  during the water years of 2002-2014 (Zhou et al., 2021), comparable to other studies in some dry areas despite different study periods (Yang et al., 2011; Wang et al., 2014; Zhang et al., 2020). Given the role of ET<sub>p</sub> in the hydrologic cycles, it is important to assess comprehensively the variations of ET<sub>p</sub> and its influencing factors, especially the interaction with surface conditions. Therefore, the overall aim of this study is to investigate the roles of meteorological variables, soil water content and vegetation growth in the ET<sub>p</sub> variation across different time scales in a humid subtropical region. The specific objectives are (1) to examine the changes in potential ET and the influencing factors over the past 3 decades or so; and (2) to quantify the multiscale impacts of major meteorological variables, soil water content and vegetation growth on ET<sub>p</sub>. The results can help improve our understanding of how evapotranspiration varies with environmental changes, thus assist the optimization of water management throughout the ecoengineering projects.

## DATA AND METHODS

### Study Area

The analysis was carried out in Guangdong province in south China (Figure 1) which has a subtropical monsoonal climate with an area around 180,000 km<sup>2</sup>. The mean annual temperature is 22°C, mean sunshine duration is around 1,745 h, and mean annual precipitation is 1,780 mm ranging from 1,300 to 2,600 mm. Previous analysis showed that precipitation was overall on the rise in the province especially in the Pearl River Delta (Fu et al., 2016; Yan et al., 2020), while evapotranspiration decreased during 1980 to 2006 (Chen et al., 2015). Alongside the global warming tendency, the province confronts with water shortages induced by population growth, extreme weather and water contamination (Zhang et al., 2011; Chen et al., 2014). Quantification of water loss through evapotranspiration is important for water availability because ET accounts for over half the annual total precipitation on average in the region (Gao, 2010).

Vegetation cover in Guangdong province was low during 1980s, until the province launched a 10-year project to plant trees primarily over the mountains starting from around 1985. At present, 59.4% of the province is covered by forests, followed by croplands (23.8%) and urban areas (12.4%); the rest are covered by grassland, shrubland, and other land use types, based on the 30-m resolution land cover data (<http://data.ess.tsinghua.edu.cn>). Elevated areas are mostly located in the north, whereas lowlands are in the south where rivers converge and flow into the South China Sea (Figure 1).

### Data Sources

We obtained meteorological measurements at 33 stations from Chinese Meteorological Administration (<http://data.cma.cn/data>), covering different land use types and altitudes (Figure 1). These meteorological variables include the maximum, minimum, and mean air temperature ( $T_{\max}$ ,  $T_{\min}$ , and  $T_{\text{avg}}$ , respectively), relative humidity (RH), wind speed ( $W_s$ ) and directions, solar radiation ( $R_s$ ), air pressure, and precipitation (P) at a monthly scale during 01/1982–12/2015. In addition, we obtained the GLEAM (Miralles et al., 2011) monthly 0.25° root-zone soil water content (SWC) data (<https://www.gleam.eu>) and the biweekly 1/12° GIMMS NDVI3g (Pinzon and Tucker, 2014) vegetation index data (<https://ecocast.arc.nasa.gov/data/pub/gimms/3g.v1>) to assist the examination of interlinkages between ET<sub>p</sub> and surface conditions. The depth of the root zone in GLEAM model is a function of the land-cover type and comprises three model layers for the fraction of tall vegetation (0–10, 10–100, and 100–250 cm), two layers for the fraction of low vegetation (0–10, 10–100 cm), and one layer for the fraction of bare soil (0–10 cm) (Martens et al., 2017). The SWC has been validated using observations from 2,325 soil moisture sensors across a broad range of ecosystems globally; unfortunately, we are not able to validate the SWC data especially the root-zone moisture throughout our study area. This could be a limitation regarding SWC accuracy but may be overcome by ensemble means of different soil moisture datasets in the future. Given that the spatial interpolation with 33 stations across the province would

likely result in large uncertainty in the ungauged areas, and accuracy of the rescaled NDVI and SWC are difficult to verify, we only analyzed the temporal dynamics and relationships using the areal average data with their original spatial resolutions.

### Calculation of ET<sub>p</sub> and the Analysis

Reference evapotranspiration based on the Penman-Monteith method (Allen et al., 1998) was calculated following Equation (1), and the results were taken as the potential ET as in other studies.

$$ET_p = \frac{0.408\Delta(R_n - G) + \gamma \frac{900}{T+273} u_2 (e_s - e_a)}{\Delta + \gamma(1 + 0.34u_2)} \quad (1)$$

$R_n$  is net radiation [ $\text{MJ m}^{-2} \text{day}^{-1}$ ] and  $G$  is soil heat flux [ $\text{MJ m}^{-2} \text{day}^{-1}$ ].  $\Delta$  is slope of saturation vapor pressure curve [ $\text{kPa}^\circ\text{C}^{-1}$ ].  $\gamma$  is psychrometric constant [ $\text{kPa}^\circ\text{C}^{-1}$ ].  $T$  is air temperature [ $^\circ\text{C}$ ].  $e_s$  and  $e_a$  is saturated and actual vapor pressure [ $\text{kPa}$ ], and their difference is the vapor pressure deficit (VPD).  $u_2$  is the wind speed at 2 m height about ground [ $\text{m s}^{-1}$ ], calculated from wind speed observed at 10 m above ground ( $W_s$ ) at the meteorological stations (Equation 2, where  $z$  is the elevation above sea level of the stations). Net radiation and soil heat flux were calculated following the procedures provided in Allen et al. (1998) and the main formulas were given in Equations (3–5).

$$u_2 = \frac{4.87W_s}{\log(67.8z - 5.42)} \quad (2)$$

$$R_n = R_{ns} - R_{nl} \quad (3)$$

$$R_{ns} = (1 - \alpha) R_s \quad (4)$$

$$R_{nl} = \sigma \left( \frac{T_{\max}^4 + T_{\min}^4}{2} \right) (0.34 - 0.14\sqrt{e_a}) \left( 1.35 \frac{R_s}{R_{so}} - 0.35 \right) \quad (5)$$

Where  $R_{ns}$  and  $R_{nl}$  are net shortwave and longwave radiation, and  $R_{so}$  is the clear-sky solar radiation.  $\alpha$  is surface albedo, prescribed as 0.23 for reference grass, and  $\sigma$  is the Stefan Boltzmann constant.  $T_{\max}$  and  $T_{\min}$  are in Kelvin degree in Equation (5).

The changing trends of ET<sub>p</sub> and the environmental variables were examined by the Mann-Kendall test. Relationships between ET<sub>p</sub> and the influencing factors were also analyzed for different seasons under dry and wet conditions by linear regression analysis. Linear trends were removed from the data series before calculating the correlation coefficients for monthly, seasonal and annual scales. For monthly scale analysis, seasonality was also removed before detrending by subtracting the climatological means from monthly data. In addition, partial correlation analysis was applied to quantify the effect of environmental

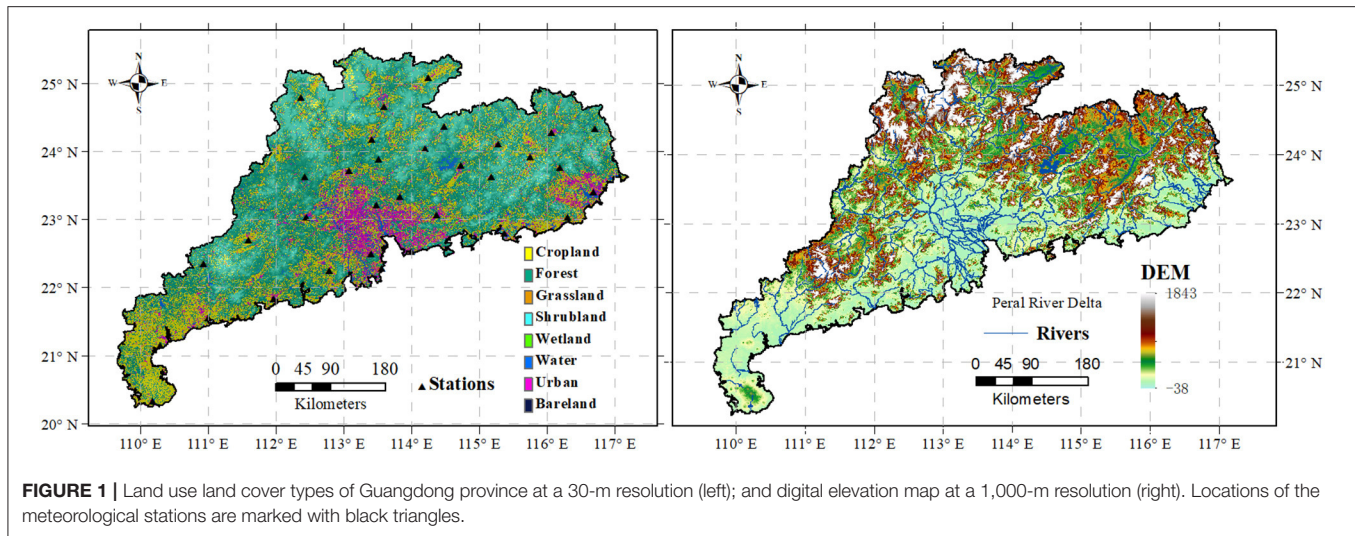


**FIGURE 1** | Land use land cover types of Guangdong province at a 30-m resolution (left); and digital elevation map at a 1,000-m resolution (right). Locations of the meteorological stations are marked with black triangles.

variables on ET<sub>p</sub> at the annual and monthly scales, which is widely used for studying the linear relationship between two variables after excluding the effect of other independent factors (Fu et al., 2015). It should be noted that the response of ET<sub>p</sub> to some factors is non-linear, especially at a sub-daily scale because of the hysteresis between ET<sub>p</sub> and these factors (Zheng et al., 2014) which is more profound in wet periods than dry periods (Wang et al., 2019b); but at a longer time scale such as daily or monthly the relationships can be linearly approximated, at least for some of the environmental factors such as radiation and VPD if not for all (Liu et al., 2014; Xu et al., 2018; Wang et al., 2019b).

## RESULTS

### Variations of ET<sub>p</sub> and the Environmental Variables

In general, the meteorological variables showed various annual dynamics, and the spatial variabilities indicated by standard deviations were also obvious (Figure 2). Precipitation has declined by  $\sim 3.7 \text{ mm yr}^{-1}$  on average over the entire period, but it decreased in the first decade or so before fluctuating irregularly. The overall trend was not statistically significant. Root-zone soil water content showed similar variation pattern with precipitation in the first decade, while it decreased sharply around 2004 and then recovered rapidly. The overall trend was not statistically significant like precipitation. Abrupt change around 2004 was also observed for ET<sub>p</sub> and R<sub>s</sub> which shared the most similar dynamic variations. Therefore, data were divided into two subperiods before and after 2004 for further analysis. Among all variables, W<sub>s</sub>, T<sub>avg</sub>, T<sub>max</sub>, T<sub>min</sub>, ET<sub>p</sub>, and NDVI saw increases across the years at a rate of 0.1 m s<sup>-1</sup>, 0.2, 0.3, 0.3 °C, 23.5 mm, and 0.012 per decade, respectively. The trends of these variables were all statistically significant with  $p < 0.05$ . Increasing trend also existed for solar radiation but the trend was not statistically significant. Overall significant and insignificant decreasing trend was observed for relative humidity ( $p < 0.05$ )

and SWC ( $p > 0.05$ ), respectively, in addition to precipitation. In this regard, the province has been getting dryer since 1980s. In particular, the increase rate over the last 11 years was 3 and 11 times the decrease rate over the first 23 years for RH and SWC, respectively (Table 1). W<sub>s</sub> and NDVI increased in both subperiods and the rate in the second subperiod was  $\sim 5$  times that in the first. In addition, the increase rate of T<sub>avg</sub>, T<sub>min</sub>, and ET<sub>p</sub> in the recent decade was only 5, 32, and 44% of that before 2004, whereas T<sub>max</sub> increased and then decreased over the two consecutive periods.

The monthly climatological variations between the two subperiods (Figure 3) were compared in different months of the year. It is observed that all variables showed clear seasonality with different peaking time. P, RH, and SWC peaked in June, and temperatures, ET<sub>p</sub> and R<sub>s</sub> peaked in July. The highest NDVI appeared in mid-autumn (October) and the lowest occurred in early spring (March). Over the two subperiods, wind speed, temperature, vegetation index and potential ET were overall higher while precipitation, relative humidity and soil water content were mostly lower over 2005–2015 than 1982–2004. However, the Wilcoxon rank sum test indicated only wind speed had statistically significant difference between the two subperiods. The comparison also shows that dynamic changes of these variables varied across months. For instance, precipitation was higher during May, June, November and December in the 2nd subperiod than the 1st, and consequently, it was the opposite for solar radiation in these months; December and January became cooler after 2005 than before 2005; vegetation greenness saw a decrease in June and October; and root-zone soil water decreased primarily in spring and increased slightly in summer and autumn. Decrease in ET<sub>p</sub> in June corresponded to increase in P, decrease in R<sub>s</sub> and NDVI.

Furthermore, we examined their interannual variations in different seasons in Figure 4 and Table 2, which shows various changing patterns. W<sub>s</sub> has increased significantly at nearly the same rate across all seasons, while RH has decreased significantly (more in spring and winter than summer and autumn). For

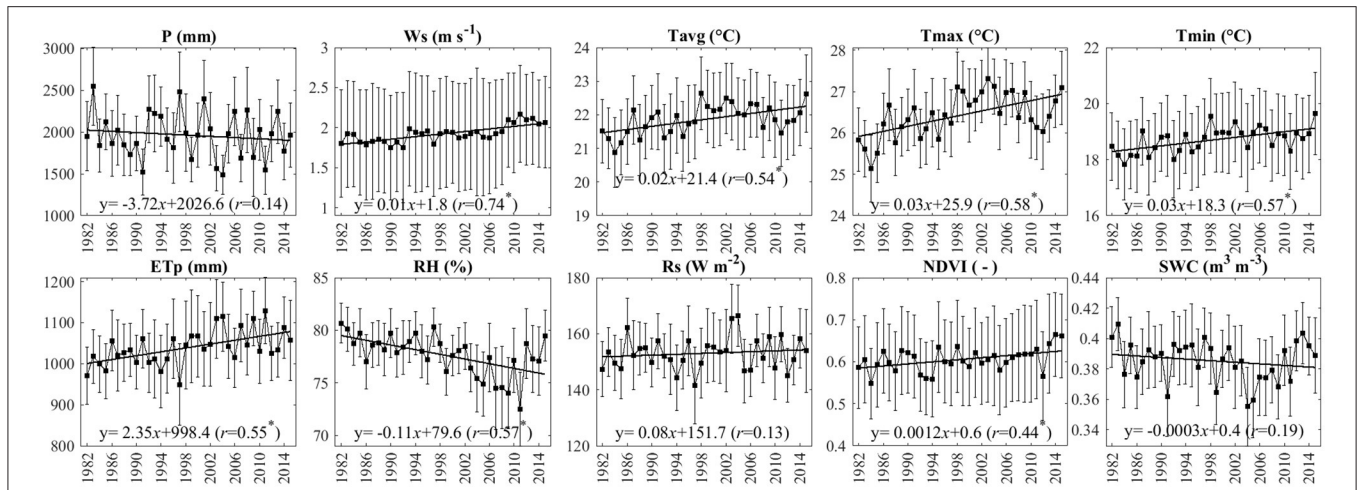


**FIGURE 2 |** Annual variations of precipitation (P), wind speed ( $W_s$ ), mean, maximum, minimum temperature ( $T_{avg}$ ,  $T_{max}$ ,  $T_{min}$ ), relative humidity (RH), solar radiation ( $R_s$ ), root-zone soil water content (SWC), normalized difference vegetation index (NDVI), and potential evapotranspiration ( $ET_p$ ). Solid straight lines infer linear trends of the relevant variables. Asterisks mark the significant trends.

**TABLE 1 |** Linear trends of the investigated variables during three different periods at the annual scale.

Variables	1982–2015		1982–2004		2005–2015		Ratio of trends
	Trend	$p$	Trend	$p$	Trend	$p$	
P	-3.7195	0.443	-8.0129	0.389	-9.5983	0.706	1.20
$W_s$	<b>0.0080</b>	0.000	<b>0.0047</b>	0.031	<b>0.0237</b>	0.006	5.04
$T_{avg}$	<b>0.0239</b>	0.001	<b>0.0496</b>	0.000	0.0023	0.948	0.05
$T_{max}$	<b>0.0309</b>	0.000	<b>0.0689</b>	0.000	-0.0107	0.787	-0.16
$T_{min}$	<b>0.0252</b>	0.001	<b>0.0404</b>	0.002	0.0128	0.728	0.32
RH	<b>-0.1114</b>	0.000	<b>-0.1173</b>	0.003	0.3363	0.106	-2.87
$R_s$	0.0765	0.457	0.3071	0.105	0.4526	0.417	1.47
NDVI	<b>0.0012</b>	0.009	<b>0.0012</b>	0.009	<b>0.0062</b>	0.024	5.17
SWC	-0.0003	0.274	-0.0003	0.274	<b>0.0033</b>	0.006	-11.00
$ET_p$	<b>2.3512</b>	0.001	<b>3.5001</b>	0.004	1.5404	0.696	0.44

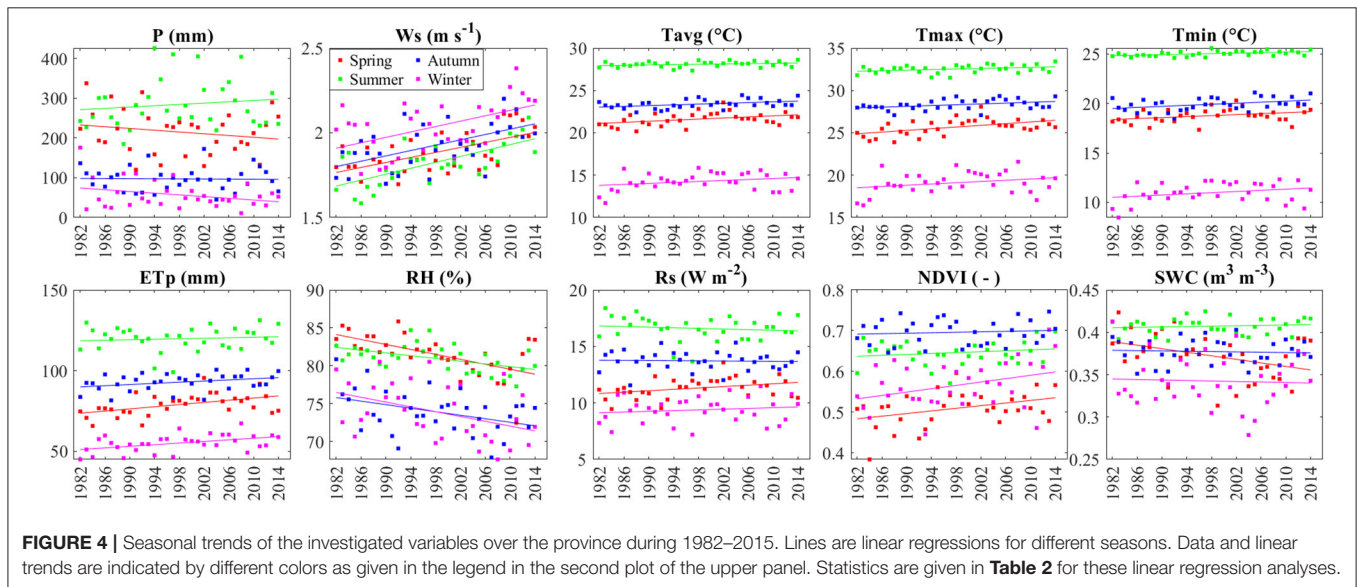
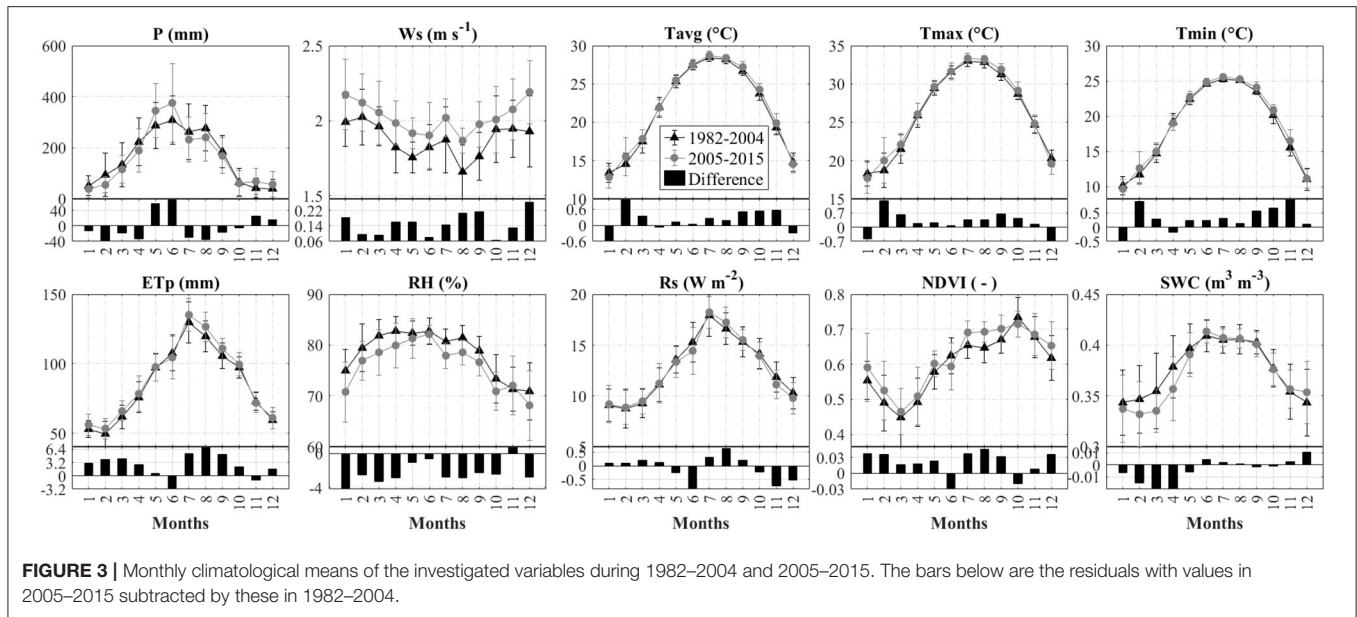
The ratio is calculated as trend over 2005–2015 divided by that over 1982–2004. In bold are those with trends statistically significant.

temperatures,  $T_{avg}$ ,  $T_{max}$ , and  $T_{min}$  have all increased across all seasons with different magnitudes, but the significant increase ( $p < 0.05$ ) appeared in spring and autumn for  $T_{avg}$ , in spring, summer and autumn for  $T_{max}$ , and in summer and autumn for  $T_{min}$ . Root-zone SWC saw an increase only in summer and the largest decrease occurred in spring ( $p < 0.05$ ), consistent with precipitation.  $R_s$  has increased in spring and winter and decreased in summer and autumn, but the trends were not statistically significant ( $p > 0.05$  for all). NDVI has increased across all seasons, and significant ( $p < 0.05$ ) and largest increase appeared in spring and winter. Seasonal  $ET_p$  trends shared the same characteristics with NDVI in terms of significant increasing trends ( $p < 0.05$ ) in spring and winter. Apart from the trends, the highs and lows of these variables appeared in different seasons, for example, precipitation, temperatures, radiation, soil water content, and  $ET_p$  were highest in summer and lowest in winter, while humidity was higher in spring and summer than autumn and winter, and NDVI was highest in autumn and lowest in

spring. This may reflect the lag relationship between vegetation growth and hydrometeorological changes.

### Multiscale Impacts of Environmental Factors on $ET_p$

The impacts of the factors on  $ET_p$  were examined by linear regression and partial correlation analysis after detrended at different time scales (and further deseasonalized for monthly scale) as stated in section Calculation of  $ET_p$  and the Analysis. **Figure 5** shows that the linear relationships were significant for P,  $T_{max}$ , RH,  $R_s$ , and SWC ( $p < 0.05$ ) at the annual scale. The strongest impact factor determined by the correlation coefficient was  $R_s$ , followed by P, RH, SWC, and  $T_{max}$  ( $r = 0.93, -0.74, -0.71, -0.59,$  and  $0.40$ , respectively). Correlation coefficients for other factors were mostly  $< 0.20$ .  $ET_p$  increased with wind speed, mean and maximum temperatures, solar radiation and vegetation greenness, while decreased with precipitation, minimum temperature, relative humidity and soil water content.



Increase in  $T_{max}$  can promote  $ET_p$  more than  $T_{avg}$  and  $T_{min}$ , which indicates that the atmospheric demand in the region would grow strongly with enhanced heatwaves.

The relationships showed different characteristics in different seasons (**Figure 6**). The regression slopes were largest in summer and lowest in winter for almost all variables, that is,  $ET_p$  was most sensitive to environmental changes in summer and least in winter. The difference between slopes in summer and winter was substantial for temperatures (e.g.,  $T_{avg}$ : 19.76 vs. 1.56), RH (16.97 vs.  $-0.04$ ), NDVI (173.00 vs. 39.26), and SWC ( $-592.02$  vs.  $-72.95$ ). Opposite effects (positive or negative) of  $W_s$  and  $T_{min}$  across different seasons were observed. Similar to the relationships at the annual scale, seasonal  $ET_p$  was also most strongly influenced by  $R_s$ , P, RH ( $R^2 > 0.50$ ,  $p < 0.05$ ).

For some influencing factors, even if the relationships were not statistically significant at the annual scale, they may be significant in different seasons, e.g.,  $T_{avg}$ ,  $T_{min}$ , and  $ET_p$  in spring and summer. Annual NDVI was not significantly related to  $ET_p$  but their relationships were significant in every season, which indicates stronger interactions between vegetation and atmospheric demand.

In **Figure 6**, the black lines are linear regressions of data pairs in all seasons, which in some way is representative of monthly relationships since the seasonal data were calculated as the mean of the 3 months in each season. The correlation coefficients ranged from 0.10 (for  $T_{min}$ ) to 0.94 (for  $R_s$ ) and were statistically significant for all except  $W_s$  and  $T_{min}$  (black numbers in **Figure 6**). The degree of influence reduced in

**TABLE 2** | Linear trends and *p*-values for the variables in **Figure 4**.

Variables	Spring		Summer		Autumn		Winter	
	Trend	<i>p</i>	Trend	<i>p</i>	Trend	<i>p</i>	Trend	<i>p</i>
P	-1.1057	0.281	0.8273	0.465	-0.0854	0.880	-1.0750	0.088
W <sub>s</sub>	<b>0.0074</b>	0.000	<b>0.0087</b>	0.000	<b>0.0079</b>	0.001	<b>0.0080</b>	0.002
T <sub>avg</sub>	<b>0.0320</b>	0.018	0.0094	0.119	<b>0.0224</b>	0.015	0.0288	0.123
T <sub>max</sub>	<b>0.0496</b>	0.002	<b>0.0165</b>	0.048	<b>0.0242</b>	0.024	0.0368	0.114
T <sub>min</sub>	0.0247	0.051	<b>0.0131</b>	0.004	<b>0.0266</b>	0.021	0.0295	0.110
RH	<b>-0.1635</b>	0.000	<b>-0.0907</b>	0.004	<b>-0.1164</b>	0.022	<b>-0.1584</b>	0.017
R <sub>s</sub>	0.0308	0.054	-0.0138	0.491	-0.0032	0.839	0.0162	0.436
NDVI	<b>0.0016</b>	0.036	0.0006	0.315	0.0003	0.610	<b>0.0021</b>	0.046
SWC	<b>-0.0010</b>	0.033	0.0001	0.505	-0.0001	0.724	-0.0001	0.790
ET <sub>p</sub>	<b>0.3355</b>	0.004	0.0749	0.589	0.1790	0.055	<b>0.2496</b>	0.008

In bold are trends with *p* < 0.05.

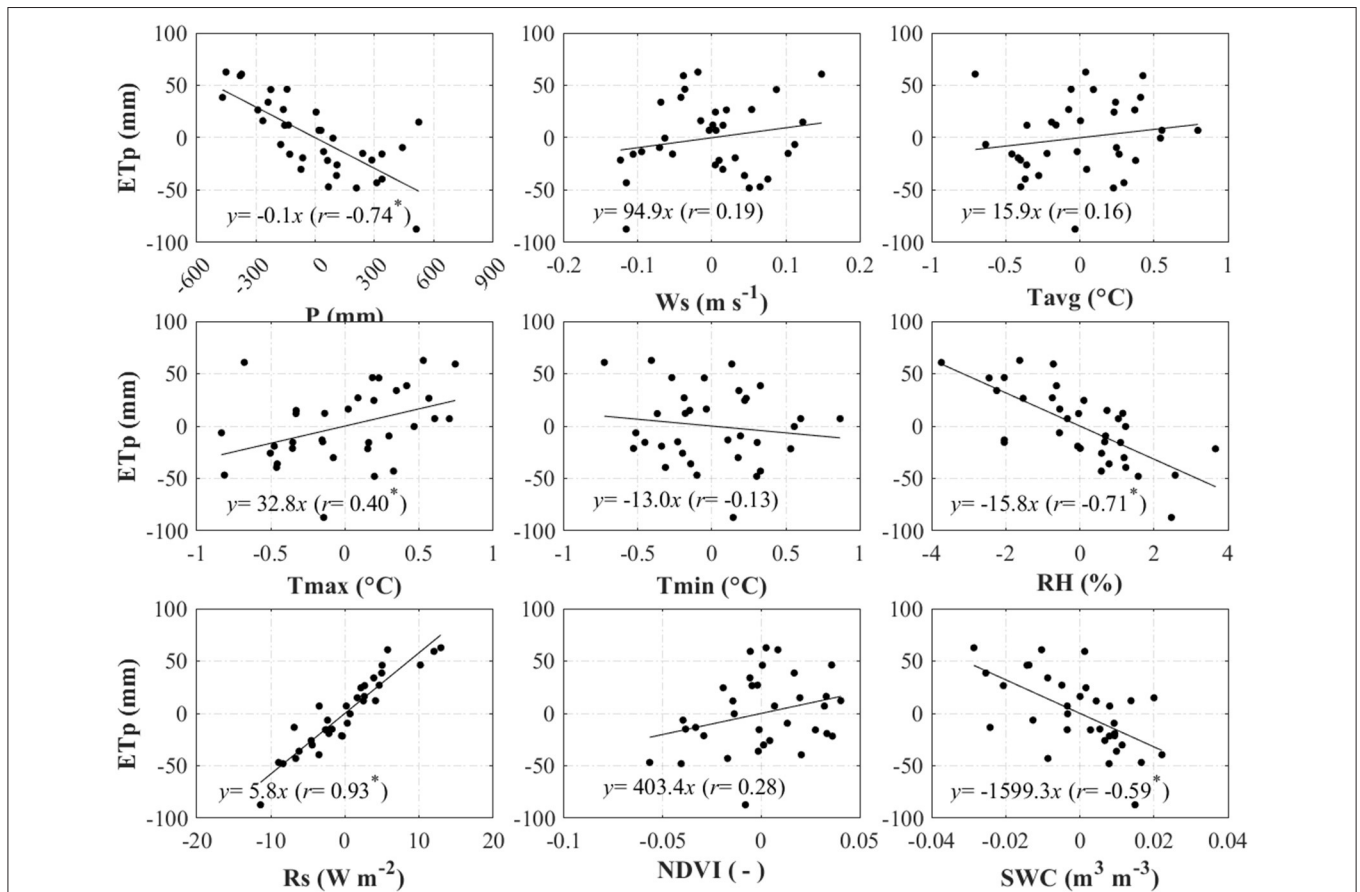


**FIGURE 5** | Scatterplots of annual ET<sub>p</sub> against different variables over the entire province. Data were detrended (for monthly, seasonal and annual data) and deseasonalized (for monthly data) before the partial correlation analysis. Asterisk infers a statistically significant linear relationship.

the sequence of R<sub>s</sub>, P, RH, T<sub>max</sub>, NDVI, SWC, and T<sub>avg</sub> with a correlation coefficient of 0.94, -0.76, -0.73, 0.61, 0.48, -0.47, and 0.40, respectively. To sum up, potential ET increased with wind speed, temperatures, solar radiation and vegetation greenness, and decreased with precipitation,

relative humidity and soil water content across different time scales.

To determine the degree of influence of each environmental variable on ET<sub>p</sub> and the interactions between these variables, we carried out partial correlation analysis which can exclude

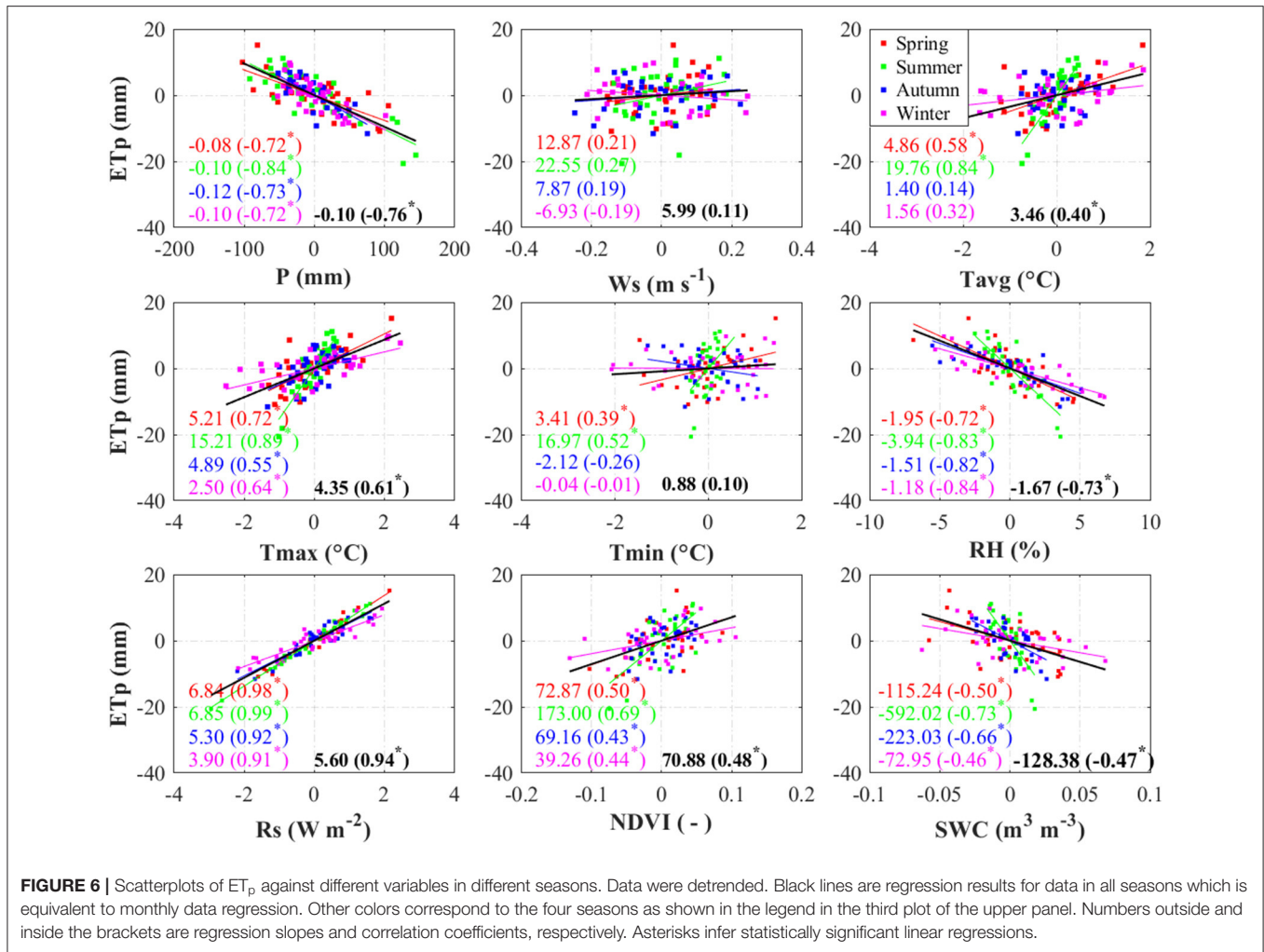


**FIGURE 6** | Scatterplots of ET<sub>p</sub> against different variables in different seasons. Data were detrended. Black lines are regression results for data in all seasons which is equivalent to monthly data regression. Other colors correspond to the four seasons as shown in the legend in the third plot of the upper panel. Numbers outside and inside the brackets are regression slopes and correlation coefficients, respectively. Asterisks infer statistically significant linear regressions.

the influence of other dependent variables when analyzing the relationship between one dependent variable and the independent variable. The partial correlation coefficients were given in **Table 3**, which showed that the environmental variables played different roles in determining ET<sub>p</sub> at different time scales. For annual data, the three most influential factors were R<sub>s</sub>, RH, and W<sub>s</sub> ( $r = 0.88, -0.87, 0.73$ , respectively, with  $p < 0.05$ ); maximum temperature also posed a significant negative effect ( $r = -0.51$ ). The influence of other environmental factors was not statistically significant. For monthly data, influences of R<sub>s</sub>, RH, and W<sub>s</sub> were also stronger than others ( $r = 0.94, -0.46$ , and  $0.33$  with  $p < 0.05$ ), and the influences of T<sub>max</sub>, T<sub>min</sub>, NDVI, and SWC were also statistically significant although correlation coefficients were relatively low. For seasonal data, R<sub>s</sub>, RH, and W<sub>s</sub> were still the strongest factors affecting ET<sub>p</sub>, and the impacts were overall stronger in summer and autumn than spring and winter. In summer, SWC also had a significant positive impact on ET<sub>p</sub> ( $r = 0.46$ ), while in autumn P and T<sub>max</sub> had significant negative impacts ( $r = -0.49$  and  $-0.41$ ) in addition to R<sub>s</sub>, RH, and W<sub>s</sub>. Therefore, in a relatively short time such as a month,

**TABLE 3** | Partial correlation coefficients ( $r$ ) between ET<sub>p</sub> and the relevant environmental variables.

	Annual	Spring	Summer	Autumn	Winter	Monthly
P	-0.24	-0.24	-0.30	<b>-0.49</b>	0.16	0.01
W <sub>s</sub>	<b>0.73</b>	<b>0.62</b>	<b>0.86</b>	<b>0.87</b>	<b>0.63</b>	<b>0.33</b>
T <sub>avg</sub>	0.34	-0.08	0.39	0.37	-0.22	-0.10
T <sub>max</sub>	<b>-0.51</b>	-0.12	-0.08	<b>-0.41</b>	0.23	<b>-0.14</b>
T <sub>min</sub>	-0.03	0.31	0.27	-0.14	0.35	<b>0.30</b>
RH	<b>-0.87</b>	<b>-0.77</b>	<b>-0.95</b>	<b>-0.87</b>	<b>-0.85</b>	<b>-0.46</b>
R <sub>s</sub>	<b>0.88</b>	<b>0.94</b>	<b>0.99</b>	<b>0.93</b>	<b>0.79</b>	<b>0.94</b>
NDVI	-0.19	0.10	-0.02	-0.26	-0.31	<b>-0.20</b>
SWC	0.19	-0.18	<b>0.46</b>	-0.19	-0.14	<b>-0.11</b>

*In bold are correlation coefficients with  $p < 0.05$ .*

ET<sub>p</sub> tends to be influenced by more environmental variables than in a relatively long time such as a season or a year; and the relationships presented both common and unique characteristics across seasons.

## DISCUSSION

### Changes in the Environment and Evaporative Demand

ET<sub>p</sub> is an important component in the simple water balance equation to indicate water deficit or surplus (Wu et al., 2019) which integrates the effects of climate and surface conditions and is often deducted by a series of environmental stress functions to estimate actual ET (Guerschman et al., 2009; Mu et al., 2011; Wang et al., 2020). Assessing the changes in ET<sub>p</sub> and its relationships with major associated influencing factors is necessary toward improving ET estimation and understanding the future climate change impacts on water resources. In this humid subtropical region, we found ET<sub>p</sub> has increased by  $\sim 2.35 \text{ mm yr}^{-1}$  during 1982–2015 ( $p < 0.05$ ). This is different from results in other part of China such as the Jiangsu province and in the Huai River Basin in eastern China, where ET<sub>p</sub> was found to decrease in general (Chu et al., 2017; Li et al., 2018). The increase in ET<sub>p</sub> was accompanied by an overall decrease in P, RH, SWC and an increase in temperatures, R<sub>s</sub>, and NDVI. Additionally, the change rate over 2005–2015 was greater than that over 1982–2004 for nearly all variables, which indicates that in the recent decade or so, the climate activities are enhanced (Yang et al., 2018) and the region gets drier and warmer in terms of rising temperature and reduced humidity, precipitation and soil water content. Down to seasons, ET<sub>p</sub> was highest in summer and lowest in winter, different from that in a province in north China (Zhang et al., 2020). The changes in ET<sub>p</sub> and the environmental variables presented different seasonal features, e.g., rainfall and SWC increased only in summer, different from the result in Pearl River basin during 1961–2007 by Gemmer et al. (2011); meanwhile, R<sub>s</sub> increased in spring and winter while decreased in summer and autumn; ET<sub>p</sub> and NDVI increased in all seasons and higher increase rate was in spring and winter. The difference in peaking time of these variables indicates the lag interactions between hydrometeorological changes and vegetation growth, which has also been revealed by analyses of climate impact on plant phenology (Estrella et al., 2015; Piao et al., 2015; Wang et al., 2019a). These detailed features are rarely reported before, but important to understand the soil-vegetation-atmosphere interactions across scales in the humid subtropical areas.

### Impacts of Environmental Changes on ET<sub>p</sub>

The impacts of environmental variables on ET<sub>p</sub> showed both similarity and difference across time scales. Namely, ET<sub>p</sub> was negatively correlated with P, RH, and SWC and positively with other variables at the annual scale, which has been found consistent across studies (Chu et al., 2017; Jerin et al., 2021; Valle Júnior et al., 2021). However, when it comes to seasons, ET<sub>p</sub> is most sensitive to environmental changes in summer and least sensitive in winter indicated by the regression slopes. This implies that the water demand in the region will increase more in summer than other seasons with a certain increase in temperatures (Wang et al., 2018; Zhang et al., 2018). In the meantime, ET<sub>p</sub> has increased the most in spring and winter, coincident

with decreased precipitation and increased temperatures, which indicates that these two seasons are more prone to water shortages with the drying and warming tendency in the region because precipitation is already the lowest in these two seasons in a year causing frequent droughts (Gao et al., 2008; Zhang et al., 2011).

When calculated following the Allen et al. (1998) method in the FAO56 paper, ET<sub>p</sub> is considered as only affected by meteorological factors because surface vegetation cover is assumed as reference grass with albedo of 0.23 and resistance of  $70 \text{ s m}^{-1}$ . While in studies carried out in southern Amazon basin in Brazil and northwest China's Qilian mountains (de Oliveira et al., 2021; Yang et al., 2021) the resultant ET<sub>p</sub> was found to have different values and trends over different land cover types, which implies that ET<sub>p</sub> is closely related to surface conditions whether or not these conditions are formulated in the reference evapotranspiration equation. If quantified by the Penman-Monteith equation with site-specific surface resistance (Chen and Dudhia, 2001; Mallick et al., 2015; Xiang et al., 2020), rather than a fixed value, ET<sub>p</sub> would be more strongly related to surface conditions including vegetation and soil moisture. We are aware that the major impact of albedo change on ET<sub>p</sub> exists in the net radiation. Albedo varies for different surfaces and for the angle of incidence. A green vegetation cover has an albedo of about 0.20–0.25, and 0.25 is recommended for natural vegetation (Seginer, 1969). Surfaces with vegetation cover would have a lower albedo than 0.25 (Chen and Dudhia, 2001). Jackson (1967) found a reduction of  $\sim 20\%$  in ET<sub>p</sub> with an increase of albedo from 0.10 to 0.25. Hua et al. (2020) discovered that the effect of albedo on ET<sub>p</sub> can be large in arid areas especially for sparsely vegetated surfaces. Our study area is in the humid subtropical south China where 60% of the surface is covered by forests, 24% by croplands, and 12% by constructed lands. The vegetation is mostly evergreen species. Therefore, the effect of albedo on ET<sub>p</sub> calculation in this study should not be as profound as in arid and sparsely vegetated areas. Nonetheless, the analysis of interaction between ET<sub>p</sub> and NDVI should also have albedo influence accounted for because albedo is associated with vegetation change. Our study shows that annual ET<sub>p</sub> varies significantly with root-zone moisture, but insignificantly with vegetation greenness, while the monthly and seasonal relationships are statistically significant. Partial correlation analysis further demonstrates the weights of each variable associated with ET<sub>p</sub> which are clearly different across time scales and in four seasons. The most weighed factors are R<sub>s</sub> and RH. Both NDVI and SWC played a negative role at the monthly scale, while SWC is more influential in summer than other seasons. In summary, through the analysis we are able to identify the role of different environmental factors in regulating potential evapotranspiration in such a humid region, and their influence on ET<sub>p</sub> varies with time scales and across different seasons. Such analysis would improve our understanding of the connections in the soil-plant-atmosphere continuum, and hence help to better manage and mitigate the climate change impacts on water resources through optimization of the surface conditions at different time of the year.

## CONCLUSIONS

This study examined the variations in potential evapotranspiration (ET<sub>p</sub>) and its relationships with the associated environmental factors across time scales. Surrogated by the reference evapotranspiration, ET<sub>p</sub> is considered to be affected solely by meteorology, however, we found in our humid subtropical region that vegetation and root-zone soil moisture also influenced ET<sub>p</sub> even though the partial correlation coefficients were relatively low (mostly within  $\pm 0.30$ , and only statistically significant at the monthly scale for both factors and in summer for soil moisture). The most influential factors are solar radiation (positive effect), followed by precipitation and relative humidity (negative effects); the impacts of other factors varied across time scales and seasons. ET<sub>p</sub> has increased the most in spring and winter, coincident with decreased precipitation and increased temperatures, which indicates that these two seasons are more prone to water shortage issues with the drying and warming tendency in the region. Moreover, changes in ET<sub>p</sub> with per unit change in environmental variables indicated by the linear regression slopes were highest in summer, which implies likely greater water demand in summer than other seasons with a warming climate. If quantified through the Penman-Monteith equation with site-specific surface resistance, ET<sub>p</sub> would be

more strongly related to vegetation and soil moisture than using reference evapotranspiration, in which situation the realization of surface conditions accounts for the vegetation change impacts on albedo and resistance.

## DATA AVAILABILITY STATEMENT

The raw data supporting the conclusions of this article will be made available by the authors, without undue reservation.

## AUTHOR CONTRIBUTIONS

JZ conceptualized the work, obtained and analyzed the data, and drafted the work. HW supervised the work and revised the paper. All authors contributed to the article and approved the submitted version.

## FUNDING

This work was financially supported by the National Key Research and Development Program of China (2021YFC3200202), the National Natural Science Foundation of China (42171020), and Guangdong Provincial Department of Science and Technology, China (2019ZT08G090).

## REFERENCES

- Adnan, R. M., Mostafa, R., Islam, A. R. M. T., Kisi, O., Kuriqi, A., and Heddami, S. (2021). Estimating reference evapotranspiration using hybrid adaptive fuzzy inferring coupled with heuristic algorithms. *Comput. Electron. Agric.* 191:106541. doi: 10.1016/j.compag.2021.106541
- Ala-aho, P., Soulsby, C., Wang, H., and Tetzlaff, D. (2017). Integrated surface-subsurface model to investigate the role of groundwater in headwater catchment runoff generation: a minimalist approach to parameterisation. *J. Hydrol.* 547, 664–677. doi: 10.1016/j.jhydrol.2017.02.023
- Allen, R. G., Luis, P. S., Dirk, R., and Smith, M. (1998). *Crop Evapotranspiration (Guidelines for Computing Crop Water Requirements)*. FAO Irrigation and Drainage Paper 56. Rome. Retrieved from: <http://www.kimberly.uidaho.edu/water/fao56/fao56.pdf>
- Beguerra, S., Vicente-Serrano, S. M., Reig, F., and Latorre, B. (2014). Standardized precipitation evapotranspiration index (SPEI) revisited: parameter fitting, evapotranspiration models, tools, datasets and drought monitoring. *Int. J. Climatol.* 34, 3001–3023. doi: 10.1002/joc.3887
- Chen, F., and Dudhia, J. (2001). Coupling an advanced land surface-hydrology model with the Penn State-NCAR MM5 modeling system. Part I: model implementation and sensitivity. *Monthly Weather Rev.* 129, 569–585. doi: 10.1175/1520-0493(2001)129<0569:CAALSH>2.0.CO;2
- Chen, X., Liu, X., Zhou, G., Han, L., Liu, W., and Liao, J. (2015). 50-year evapotranspiration declining and potential causations in subtropical Guangdong province, southern China. *Catena* 128, 185–194. doi: 10.1016/j.catena.2015.02.001
- Chen, Z., Zhu, Z., Yin, L., Wei, S., and Deng, L. (2014). The changing water quality characteristics from urban drinking water sources in Guangdong, China. *Water Resour. Manage.* 29, 987–1002. doi: 10.1007/s11269-014-0855-0
- Chu, R., Li, M., Shen, S., Islam, A. R. M. T., Cao, W., Tao, S., et al. (2017). Changes in reference evapotranspiration and its contributing factors in Jiangsu, a major economic and agricultural province of Eastern China. *Water* 9, 1–20. doi: 10.3390/w9070486
- de Oliveira, R. G., Valle Júnior, L. C. G., da Silva, J. B., Espíndola, D. A. L. F., Lopes, R. D., Nogueira, J. S., et al. (2021). Temporal trend changes in reference evapotranspiration contrasting different land uses in southern Amazon basin. *Agric. Water Manage.* 250:106815. doi: 10.1016/j.agwat.2021.106815
- Duethmann, D., and Blöschl, G. (2018). Why has catchment evaporation increased in the past 40 years? A data-based study in Austria. *Hydrol. Earth Syst. Sci. Discuss.* 22, 5143–5158. doi: 10.5194/hess-2018-129
- Estrella, N., Estrella, N., and Menzel, A. (2015). Responses of leaf colouring in four deciduous tree species to climate and weather in Germany. *Clim. Res.* 32, 253–267. doi: 10.3354/cr032253
- Fisher, J. B., Whittaker, R. J., and Malhi, Y. (2011). ET come home: potential evapotranspiration in geographical ecology. *Glob. Ecol. Biogeogr.* 20, 1–18. doi: 10.1111/j.1466-8238.2010.00578.x
- Fu, S., Li, D., Sun, J., Si, D., Ling, J., and Tian, F. (2016). A 31-year trend of the hourly precipitation over South China and the underlying mechanisms. *Atmos. Sci. Lett.* 17, 216–222. doi: 10.1002/asl.645
- Fu, Y. H., Piao, S., Vitasse, Y., Zhao, H., De Boeck, H. J., Liu, Q., et al. (2015). Increased heat requirement for leaf flushing in temperate woody species over 1980–2012: effects of chilling, precipitation and insolation. *Glob. Change Biol.* 21, 2687–2697. doi: 10.1111/gcb.12863
- Gao, M., Qin, Z., Zhang, H., Lu, L., Zhou, X., and Yang, X. (2008). Remote sensing of agro-droughts in Guangdong Province of China using MODIS satellite data. *Sensors* 8, 4687–4708. doi: 10.3390/s8084687
- Gao, X. (2010). *Actual Evapotranspiration in the Pearl River Basin: Estimation, Spatio-Temporal Variations and Climatic Sensitivities*. The Chinese University of Hong Kong. doi: 10.1017/S0033291717001520
- Gemmer, M., Fischer, T., Jiang, T., Su, B., and Liu, L. L. (2011). Trends in precipitation extremes in the Zhujiang River basin, South China. *J. Clim.* 24, 750–761. doi: 10.1175/2010JCLI3717.1
- Guerschman, J. P., Van Dijk, A. I. J. M., Mattersdorf, G., Beringer, J., Hutley, L. B., Leuning, R., et al. (2009). Scaling of potential evapotranspiration with MODIS data reproduces flux observations and catchment water balance observations across Australia. *J. Hydrol.* 369, 107–119. doi: 10.1016/j.jhydrol.2009.02.013
- Hua, D., Hao, X., Zhang, Y., and Qin, J. (2020). Uncertainty assessment of potential evapotranspiration in arid areas, as estimated by the Penman-Monteith method. *J. Arid Land* 12, 166–180. doi: 10.1007/s40333-020-0093-7
- Jackson, R. J. (1967). The effect of slope, aspect and albedo on potential evapotranspiration from hillslopes and catchments. *J. Hydrol.* 6, 60–69.
- Jerin, J. N., Islam, H. M. T., Islam, A. R. M. T., Shahid, S., Hu, Z., Badhan, M. A., et al. (2021). Spatiotemporal trends in reference evapotranspiration

- and its driving factors in Bangladesh. *Theoret. Appl. Climatol.* 144, 793–808. doi: 10.1007/s00704-021-03566-4
- Jiao, W., Wang, L., Smith, W. K., Chang, Q., Wang, H., and D'Odorico, P. (2021). Observed increasing water constraint on vegetation growth over the last three decades. *Nat. Commun.* 12, 1–9. doi: 10.1038/s41467-021-24016-9
- Kirkham, M. B. (2014). "Potential evapotranspiration," in *Principles of Soil and Plant Water Relations*, ed C. Janco (Waltham: Elsevier), 501–514. doi: 10.1016/b978-0-12-420022-7.00028-8
- Li, M., Chu, R., Shen, S., and Islam, A. R. M. T. (2018). Quantifying climatic impact on reference evapotranspiration trends in the Huai River Basin of Eastern China. *Water* 10:144. doi: 10.3390/w10020144
- Liu, B., Zhao, W., Wen, Z., and Zhang, Z. (2014). Response of water and energy exchange to the environmental variable in a desert-oasis wetland of Northwest China. *Hydrol. Process.* 28, 6098–6112. doi: 10.1002/hyp.10098
- Lu, J., Sun, G., McNulty, S. G., and Amaty, D. M. (2005). A comparison of six potential evapotranspiration methods for regional use in the southeastern United States. *J. Am. Water Resour. Assoc.* 41, 621–633. doi: 10.1111/j.1752-1688.2005.tb03759.x
- Mallick, K., Boegh, E., Trebs, I., Alfieri, J. G., Kustas, W. P., Prueger, J. H., et al. (2015). Reintroducing radiometric surface temperature into the Penman-Monteith formulation. *Water Resour. Res.* 51, 6214–6243. doi: 10.1002/2014WR016106
- Mallick, K., Jarvis, A., Fisher, J. B., Tu, K. P., Boegh, E., and Niyogi, D. (2013). Latent heat flux and canopy conductance based on Penman-Monteith, Priestley-Taylor equation, and Bouchet's complementary hypothesis. *J. Hydrometeorol.* 14, 419–442. doi: 10.1175/JHM-D-12-0117.1
- Martens, B., Miralles, D. G., Lievens, H., Van Der Schalie, R., De Jeu, R. A. M., Fernández-Prieto, D., et al. (2017). GLEAM v3: Satellite-based land evaporation and root-zone soil moisture. *Geosci. Model Dev.* 10, 1903–1925. doi: 10.5194/gmd-10-1903-2017
- Miralles, D. G., De Jeu, R. A. M., Gash, J. H., Holmes, T. R. H., and Dolman, A. J. (2011). Magnitude and variability of land evaporation and its components at the global scale. *Hydrol. Earth Syst. Sci.* 15, 967–981. doi: 10.5194/hess-15-967-2011
- Monteith, J. L. (1965). *Evaporation and Environment*. Swansea: Symposia of the Society for Experimental Biology.
- Mu, Q., Heinsch, F. A., Zhao, M., and Running, S. W. (2007). Development of a global evapotranspiration algorithm based on MODIS and global meteorology data. *Remote Sens. Environ.* 111, 519–536. doi: 10.1016/j.rse.2006.07.007
- Mu, Q., Zhao, M., and Running, S. W. (2011). Improvements to a MODIS global terrestrial evapotranspiration algorithm. *Remote Sens. Environ.* 115, 1781–1800. doi: 10.1016/j.rse.2011.02.019
- Oudin, L., Hervieu, F., Michel, C., Perrin, C., Andréassian, V., Anctil, F., et al. (2005). Which potential evapotranspiration input for a lumped rainfall-runoff model? Part 2 - Towards a simple and efficient potential evapotranspiration model for rainfall-runoff modelling. *J. Hydrol.* 303, 290–306. doi: 10.1016/j.jhydrol.2004.08.026
- Piao, S., Tan, J., Chen, A., Fu, Y. H., Ciais, P., Liu, Q., et al. (2015). Leaf onset in the northern hemisphere triggered by daytime temperature. *Nat. Commun.* 6:7911. doi: 10.1038/ncomms7911
- Pinzon, J. E., and Tucker, C. J. (2014). A non-stationary 1981–2012 AVHRR NDVI3g time series. *Remote Sens.* 6, 6929–6960. doi: 10.3390/rs6086929
- Priestley, C. H. B., and Taylor, R. J. (1972). *On the Assessment of Surface Heat Flux and Evaporation Using Large-Scale Parameters*. Retrieved from: [https://journals.ametsoc.org/view/journals/mwre/100/2/1520-0493\\_1972\\_100\\_0081\\_otaosh\\_2\\_3\\_co\\_2.xml](https://journals.ametsoc.org/view/journals/mwre/100/2/1520-0493_1972_100_0081_otaosh_2_3_co_2.xml)
- Rodell, M., Houser, P. R., Jambor, U., Gottschalck, J., Mitchell, K., Meng, C. J., et al. (2004). The global land data assimilation system. *Bull. Am. Meteorol. Soc.* 85, 381–394. doi: 10.1175/BAMS-85-3-381
- Rosenberg, N. J. (1974). *Microclimate: The Biological Environment*. New York, NY: John Wiley and Sons, Inc.
- Salam, R., and Islam, A. R. M. T. (2020). Potential of RT, bagging and RS ensemble learning algorithms for reference evapotranspiration prediction using climatic data-limited humid region in Bangladesh. *J. Hydrol.* 590:125241. doi: 10.1016/j.jhydrol.2020.125241
- Seginer, I. (1969). The effect of albedo on the evapotranspiration rate. *Agric. Meteorol.* 6, 5–31. doi: 10.1016/0002-1571(69)90031-4
- Thorntwaite, C. W. (1948). An approach toward a rational classification of climate. *Geograph. Rev.* 38:55. doi: 10.2307/210739
- Valle Júnior, L. C. G., Do Vourlitis, G. L., Curado, L. F. A., Palácios, R. S., Nogueira, J. S., Lobo, F. A., et al. (2021). Evaluation of fao-56 procedures for estimating reference evapotranspiration using missing climatic data for a Brazilian tropical savanna. *Water* 13, 1–17. doi: 10.3390/w13131763
- Vicente-Serrano, S. M., Beguería, S., and López-Moreno, J. I. (2010). A multiscale drought index sensitive to global warming: the standardized precipitation evapotranspiration index. *J. Clim.* 23, 1696–1718. doi: 10.1175/2009JCLI2909.1
- Wang, H., Guan, H., Liu, N., Soulsby, C., Tetzlaff, D., and Zhang, X. (2020). Improving the Jarvis-type model with modified temperature and radiation functions for sap flow simulations. *J. Hydrol.* 587:124981. doi: 10.1016/j.jhydrol.2020.124981
- Wang, H., Tetzlaff, D., Buttle, J., Carey, S. K., Laudon, H., McNamara, J. P., et al. (2019a). Climate-phenology-hydrology interactions in northern high latitudes: assessing the value of remote sensing data in catchment ecohydrological studies. *Sci. Tot. Environ.* 656, 19–28. doi: 10.1016/j.scitotenv.2018.11.361
- Wang, H., Tetzlaff, D., and Soulsby, C. (2019b). Hysteretic response of sap flow in Scots pine (*Pinus sylvestris*) to meteorological forcing in a humid low-energy headwater catchment. *Ecohydrology* 12:e2125. doi: 10.1002/eco.2125
- Wang, X. M., Liu, H. J., Zhang, L. W., and Zhang, R. H. (2014). Climate change trend and its effects on reference evapotranspiration at Linhe Station, Hetao Irrigation District. *Water Sci. Eng.* 7, 250–266. doi: 10.3882/j.issn.1674-2370.2014.03.002
- Wang, Z., Zhong, R., Lai, C., Zeng, Z., Lian, Y., and Bai, X. (2018). Climate change enhances the severity and variability of drought in the Pearl River Basin in South China in the 21st century. *Agric. For. Meteorol.* 249, 149–162. doi: 10.1016/j.agrformet.2017.12.077
- Wen, X., Yang, B., Sun, X., and Lee, X. (2016). Evapotranspiration partitioning through *in-situ* oxygen isotope measurements in an oasis cropland. *Agric. Forest Meteorol.* 230–231, 89–96. doi: 10.1016/j.agrformet.2015.12.003
- Wu, X., Guo, W., Liu, H., Li, X., Peng, C., Allen, C. D., et al. (2019). Exposures to temperature beyond threshold disproportionately reduce vegetation growth in the northern hemisphere. *Nat. Sci. Rev.* 6, 786–795. doi: 10.1093/nsr/nwy158
- Xiang, K., Li, Y., Horton, R., and Feng, H. (2020). Similarity and difference of potential evapotranspiration and reference crop evapotranspiration – a review. *Agric. Water Manage.* 232. [Epub ahead of print]. doi: 10.1016/j.agwat.2020.106043
- Xu, S., Yu, Z., Yang, C., Ji, X., and Zhang, K. (2018). Trends in evapotranspiration and their responses to climate change and vegetation greening over the upper reaches of the Yellow River Basin. *Agric. Forest Meteorol.* 263, 118–129. doi: 10.1016/j.agrformet.2018.08.010
- Yan, M., Chan, J. C. L., and Zhao, K. (2020). Impacts of urbanization on the precipitation characteristics in Guangdong Province, China. *Adv. Atmos. Sci.* 37, 696–706. doi: 10.1007/s00376-020-9218-3
- Yang, L., Feng, Q., Adamowski, J. F., Alizadeh, M. R., Yin, Z., Wen, X., et al. (2021). The role of climate change and vegetation greening on the variation of terrestrial evapotranspiration in northwest China's Qilian Mountains. *Sci. Total Environ.* 759, 143532. doi: 10.1016/j.scitotenv.2020.143532
- Yang, L. E., Chan, F. K. S., and Scheffran, J. (2018). Climate change, water management and stakeholder analysis in the Dongjiang River basin in South China. *Int. J. Water Resour. Dev.* 34, 166–191. doi: 10.1080/07900627.2016.1264294
- Yang, Y., Roderick, M. L., Zhang, S., McVicar, T. R., and Donohue, R. J. (2019). Hydrologic implications of vegetation response to elevated CO<sub>2</sub> in climate projections. *Nat. Clim. Change* 9, 44–48. doi: 10.1038/s41558-018-0361-0
- Yang, Z., Liu, Q., and Cui, B. (2011). Distribution spatiale et variation temporelle de l'évapotranspiration de référence pendant la période 1961–2006 dans le bassin du Fleuve Jaune, en Chine. *Hydrol. Sci. J.* 56, 1015–1026. doi: 10.1080/02626667.2011.590810
- Zhan, S., Song, C., Wang, J., Sheng, Y., and Quan, J. (2019). A global assessment of terrestrial evapotranspiration increase due to surface water area change. *Earth's Future* 7, 266–282. doi: 10.1029/2018EF001066
- Zhang, F., Liu, Z., Zhangzhong, L., Yu, J., Shi, K., and Yao, L. (2020). Spatiotemporal distribution characteristics of reference evapotranspiration in Shandong province from 1980 to 2019. *Water* 12, 1–16. doi: 10.3390/w12123495
- Zhang, H., and Wang, L. (2021). Analysis of the variation in potential evapotranspiration and surface wet conditions in the Hancang River Basin, China. *Sci. Rep.* 11:8607. doi: 10.1038/s41598-021-88162-2

- Zhang, Q., Li, J., Gu, X., and Shi, P. (2018). Is the Pearl River basin, China, drying or wetting? Seasonal variations, causes and implications. *Glob. Planet. Change.* 166, 48–61. doi: 10.1016/j.gloplacha.2018.04.005
- Zhang, Q., Zhang, W., Chen, Y. D., and Jiang, T. (2011). Flood, drought and typhoon disasters during the last half-century in the Guangdong province, China. *Nat. Hazards.* 57, 267–278. doi: 10.1007/s11069-010-9611-9
- Zhang, Y., Kong, D., Gan, R., Chiew, F. H. S., McVicar, T. R., Zhang, Q., et al. (2019). Coupled estimation of 500 m and 8-day resolution global evapotranspiration and gross primary production in 2002–2017. *Remote Sens. Environ.* 222, 165–182. doi: 10.1016/j.rse.2018.12.031
- Zheng, H., Wang, Q., Zhu, X., Li, Y., and Yu, G. (2014). Hysteresis responses of evapotranspiration to meteorological factors at a diel timescale: patterns and causes. *PLoS ONE* 9:e98857. doi: 10.1371/journal.pone.0098857
- Zhou, R., Wang, H., Duan, K., and Liu, B. (2021). Diverse responses of vegetation to hydroclimate across temporal scales in a humid subtropical region. *J. Hydrol. Region. Stud.* 33:100775. doi: 10.1016/j.ejrh.2021.100775

**Conflict of Interest:** The authors declare that the research was conducted in the absence of any commercial or financial relationships that could be construed as a potential conflict of interest.

**Publisher's Note:** All claims expressed in this article are solely those of the authors and do not necessarily represent those of their affiliated organizations, or those of the publisher, the editors and the reviewers. Any product that may be evaluated in this article, or claim that may be made by its manufacturer, is not guaranteed or endorsed by the publisher.

Copyright © 2022 Wang and Zheng. This is an open-access article distributed under the terms of the Creative Commons Attribution License (CC BY). The use, distribution or reproduction in other forums is permitted, provided the original author(s) and the copyright owner(s) are credited and that the original publication in this journal is cited, in accordance with accepted academic practice. No use, distribution or reproduction is permitted which does not comply with these terms.